Article:

Takahagi, K. orcid.org/0009-0003-7592-4216 and Tennant, A. orcid.org/0000-0003-3973-7571 (2025) A dual-polarised nonreciprocal electromagnetic metasurface. Electronics Letters, 61 (1). e70177. ISSN 0013-5194

https://doi.org/10.1049/ell2.70177

Electronics Letters

LETTER OPEN ACCESS

A Dual-Polarised Nonreciprocal Electromagnetic Metasurface

Kazuhiro Takahagi | Alan Tennant

School of Electrical and Electronic Engineering, The University of Sheffield, Portobello Centre, Sheffield, UK

Correspondence: Kazuhiro Takahagi (Ktakahagi1@Sheffield.ac.uk)

Received: 28 November 2024 | **Revised:** 30 January 2025 | **Accepted:** 8 February 2025

Funding: This work was supported by the University of Sheffield (Institution code: J009).

ABSTRACT

The application of electromagnetic materials to mobile systems and other platforms requiring complex utilization of radio waves necessitates compatibility with various polarizations. For nonreciprocal metasurfaces that support unidirectional propagation, achieving dual polarization (vertical and horizontal) presents significant design challenges. This study proposes a simple structure for dual-polarization nonreciprocal metasurfaces and presents theoretical and experimental analyses of its performance. As a result, a dual-polarization nonreciprocal metasurface exhibiting high-pass filter characteristics at C-band is realised by incorporating ferrite into a strip line lattice structure, achieving an isolation of 7 dB.

1 | Introduction

In recent years, a paradigm shift has extended beyond 5G and 6G communications to encompass comprehensive radio wave management [1]. Efficient electromagnetic wave use has driven technologies such as electromagnetic metasurfaces for reflection and absorption [2], metamaterials for compact and wideband bandpass filters [3], and reconfigurable intelligent surfaces (RISs) for antenna design [4]. Electromagnetic metasurfaces enable specific behaviours through periodic surface patterns [5], with research spanning broadband absorbers [6] and tunable reflection control materials [7].

Among these advancements, nonreciprocal metasurfaces uniquely enable unidirectional wave propagation. Unlike conventional frequency-selective filters that rely on frequency or polarization, nonreciprocal metasurfaces filter waves by arrival direction [8–10]. Prior studies explored spatial nonreciprocity using array antennas and amplifiers with unidirectional gain [8] or magnetic materials for propagation control [9]. Despite progress, controlling the propagation direction of plane waves with identical frequencies and polarizations remains a key challenge. Realizing spatial nonreciprocity with robust environmental resistance is critical, as such surfaces serve as essential electromagnetic control components, analogous to circuit isolation.

Our group has proposed simplified metasurfaces embedded with magnetic materials [11] and developed corresponding design methodologies [12]. However, earlier nonreciprocal metasurfaces primarily targeted single polarizations aligned with the material's magnetization direction. To address the complexities of electromagnetic environments, dual-polarization compatibility is crucial. This study demonstrates the theoretical and experimental feasibility of extending nonreciprocity to dual-polarization configurations.

2 | Nonreciprocity Methodology

The proposed method achieves nonreciprocity by combining the rotational propagation characteristics of cylindrical ferrite materials with the filtering properties of periodic metallic structures [12]. Table 1 compares prior research on nonreciprocal

TABLE 1 | Comparison with previous studies.

	This work	[8]	[9]	[10]
Active/Passive	P	A	P	P
Mag./Non-mag.	M	N	M	N
Polarization dependence	No (V/H)	Yes (V)	Yes (Circle)	Yes (Circle)

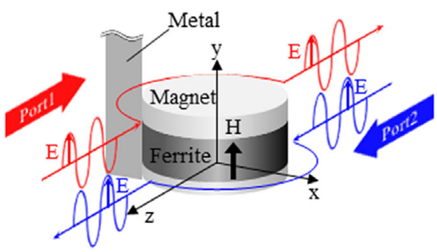

FIGURE 1 | Ferrite behaviour and nonreciprocity.

metasurfaces with the method proposed here. Key considerations in nonreciprocity research include whether passive or active elements are used and whether magnetic materials are involved. Previous studies explored nonreciprocity using antenna pairs and amplifiers [8], magnetic materials [9], and distinct responses for various polarizations [10]. However, these methods depend on the shape of the antenna or ferrite and typically achieve nonreciprocity for specific polarizations. In contrast, the proposed approach achieves consistent nonreciprocity across multiple polarizations. Previously, nonreciprocity with magnetic materials was often realized by aligning the electromagnetic wave propagation with the magnetization direction of the material, using anisotropic permeability to control rotation [9, 13]. These methods require precise rotation angle settings in the magnetic material, restricting design flexibility.

In contrast, our method integrates the rotational propagation properties of ferrite with the transmission and reflection control afforded by widely studied metallic strips or patch arrays. As shown in Figure 1, the magnetization direction of the ferrite aligns with the y-axis, perpendicular to the z-axis (propagation direction), causing rotation in the zx-plane. Unlike conventional methods, this approach eliminates the need to account for the rotation angle. By placing the ferrite near metallic strip structures, it becomes possible to selectively utilize the strip line characteristics, achieving unidirectional propagation. The primary advantage of this method is its ability to impart nonreciprocity to existing transmission/reflection characteristics of metallic patch arrays by simply incorporating magnetic materials. However, in its current state, the nonreciprocal effect is limited to vertical polarization with an electric field aligned along the magnetization axis.

3 | Design for Dual-Polarization Compatibility

Previously reported nonreciprocal metasurfaces using one-dimensional strip lines and magnetic materials achieved high pass filtering with nonreciprocal characteristics for vertical polarization [12] (Figure 2a). In Figure 2a, propagation from Port 1

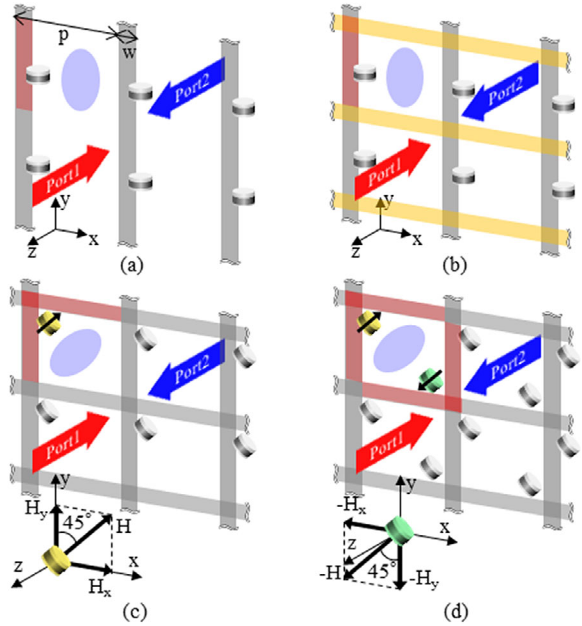

FIGURE 2 | Nonreciprocal structure, (a) conventional, (b) horizontal strip line added, (c) 1 cell 1 ferrite for both polarizations, and (d) 1 cell 2 ferrite for both polarizations.

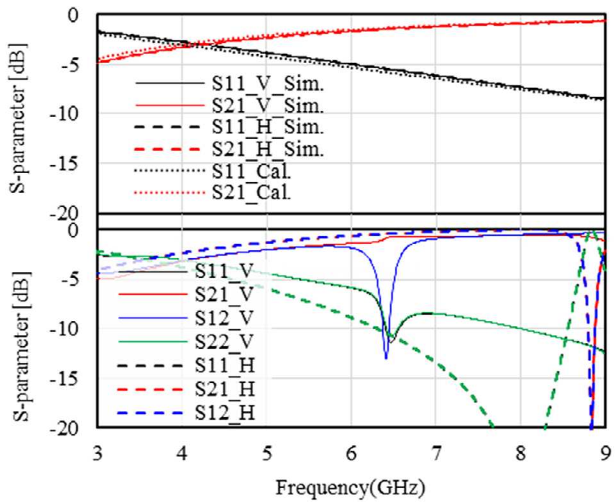

FIGURE 3 | Analysis results when adding horizontal strips: (Top) no ferrite, (bottom) with vertical ferrite.

interacts with the red metallic strip area, while propagation from Port 2 affects the blue void regions. To achieve dual-polarization compatibility, the first step involves arranging the metallic strip lines into a lattice structure to provide high-pass filtering for both vertical and horizontal polarizations (Figure 2b). By adding strip lines along the x-axis, as shown by the yellow lines in Figure 2b, similar high-pass filter characteristics are imparted to horizontal polarization. Figure 3 (top) shows the characteristics of the lattice strip line structure without ferrite. The inductance component of the linear metallic strip lines is described by transmission line theory as follows [14]:

$$X_L \approx \frac{p\cos\theta}{\lambda}\left\{1n\,\frac{2p}{\pi w} + \frac{1}{2}\left(3 - 2\cos^2\theta\right)\left(\frac{p}{\lambda}\right)^2\right\} \qquad (1)$$

where l represents wavelength and q denotes incident angle. For comparison, infinite-plane analysis of this structure was conducted using CST Studio Suite's F-solver. The calculated S-parameters, shown in Figure 3 (top), agree with electromagnetic simulations of vertical and horizontal polarizations, confirming the validity of the model. Based on a parametric study to achieve nonreciprocal behaviour at the 6 GHz band, the line width w and pitch p were set to 2 and 20 mm, respectively.

Next, Figure 3 (bottom) presents simulations with vertically placed ferrite in the structure shown in Figure 2b. Ferrite parameters include a 7 mm diameter, 2 mm height, relative permittivity of 15, relative permeability of 1.1, saturation magnetization of 1600 Gauss, and magnetizing field of 650 Gauss. Results show the nonreciprocal effect for vertical polarization achieves isolation over −10 dB at 6.3 GHz, consistent with single-polarization results, while horizontal polarization retains high-pass characteristics, marking progress toward dual-polarization compatibility. To achieve nonreciprocity for both polarizations, Figure 2c tilts ferrite 45° in the xy-plane, positioning it in void corners to utilize rotational propagation on metallic strips. Tilting applies equal magnetizing fields along x and y axes ($H_x = H_y = H/\sqrt{2}$). To enhance nonreciprocal characteristics, Figure 2d proposes a design with ferrite magnetized in opposite diagonal directions.

4 | Experimental results

Experimental results for the structures shown in Figure 2c,d are presented using antenna pairs. It has been confirmed that the nonreciprocal characteristics of our proposed structure can be verified with minimal configurations, even for infinite planes [11]. The experiments employed a 2 × 2-cell sample. To eliminate edge effects, a metal plate with an opening corresponding to the sample size was placed around the sample's installation point between the antenna pair.

First, the results for a structure with one ferrite per cell are shown in Figure 4a. The top and bottom plots correspond to vertical and horizontal polarization, respectively. Identical nonreciprocal characteristics were observed for both polarizations around 6.3 GHz, consistent with single-polarization results. However, the isolation level was approximately −4 dB.

Next, the results for the improved structure with two ferrites per cell are shown in Figure 4b. While the nonreciprocal frequency remained unchanged, the isolation improved to approximately −7 dB, demonstrating enhanced performance. Electromagnetic simulation results for comparison are included, showing good agreement with the experimental data. In the experiment, a 20 mm unit cell was arranged in a 2 × 2 configuration, resulting in a 40 mm sample size. The sample was positioned at the centre of a 50 mm square hole in a metal plate to suppress diffraction. However, interference between the sample and the plate was observed. The simulation results, shown as black lines in Figures 4 and 5, revealed band-stop effects near 5.3 and 7 GHz. At 5.3 GHz, outside the ferrite's operating range, S21 and S12 dips were observed. At 7 GHz, within the ferrite's range, nonreciprocity was confirmed. The two observed peaks result from finite size effects; infinite samples exhibit a single peak. The electric field distribution at 6.3 GHz, where nonreciprocity was achieved, is shown in Figure 5.

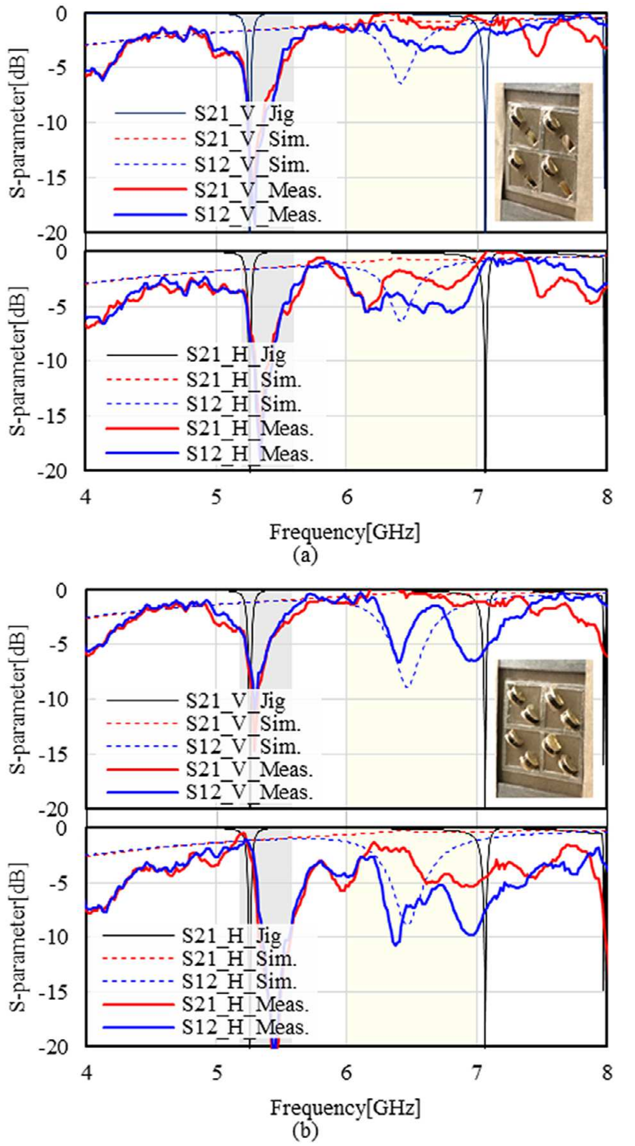

FIGURE 4 | Comparison of experimental and analytical results: (a) Vertical characteristics (top) and horizontal characteristics (bottom) for 1 ferrite in 1 cell; (b) Vertical characteristics (top) and horizontal characteristics (bottom) for 2 ferrites in 1 cell.

It confirms the correct rotational propagation characteristics for both vertical and horizontal polarizations, even with ferrite positioned diagonally. Furthermore, propagation from Port 2 was effectively blocked by the voids. The reduced isolation compared to single-polarization results is attributed to the relatively weaker magnetizing field strength, which can be addressed by increasing the field intensity. These findings validate the feasibility of a novel structure that can impart nonreciprocal characteristics to both vertical and horizontal polarizations in a simplified, retrofittable configuration.

5 | Conclusion

Nonreciprocal metasurfaces capable of handling both vertical and horizontal polarizations are critically needed for use in complex electromagnetic environments. This study demonstrated

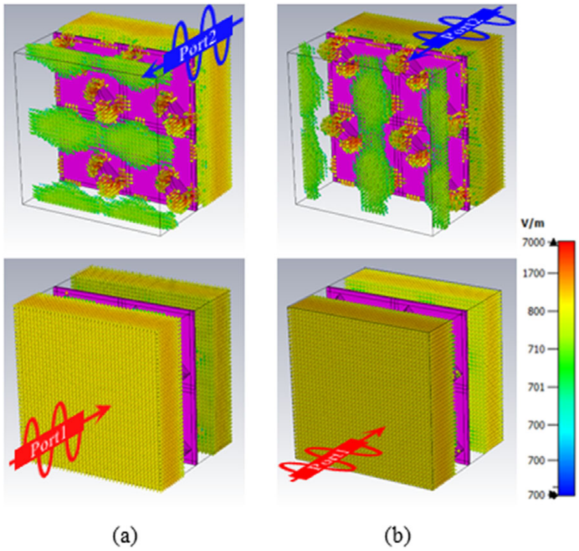

FIGURE 5 | Electric field distribution analysis results at 6.3 GHz: (a) Vertical polarization and (b) horizontal polarization.

theoretical and experimental results for a simplified structure capable of accommodating both polarizations. We extended the nonreciprocity of previously vertical-polarization-only metasurfaces to include horizontal polarization. A structure operating for both polarizations was proposed, achieving this without affecting the operational frequency band. The findings indicate the feasibility of applying this technology to arbitrary dual-polarization metallic array structures. Future directions include expanding its application to various structures and enhancing performance further.

Author Contributions

Kazuhiro Takahagi: conceptualization; data curation; formal analysis; methodology; project administration; validation; visualization; and writing – original draft preparation. **Alan Tennant:** funding acquisition; investigation, resources; software; supervision; and writing – review and editing.

Conflicts of Interest

The authors declare no conflicts of interest.

Data Availability Statement

The data that support the findings of this study are available from the corresponding author upon reasonable request.

References

1. Y. Posherstnik, E. R. Rocksvald, B. Lussier, and M. Makowski, "Framework for Interoperable Command & Control of Joint Electromagnetic Spectrum Operations," in *Proceedings of the MILCOM 2019 - 2019 IEEE Military Communications Conference (MILCOM)*, Norfolk, VA, USA, (IEEE, 2019), 28–33.

2. A. K. Rathor, R. Porwal, G. Samanta, and M. V. D. Nair, "Dual-Band Metasurface Absorber for Wi-Fi Shielding Applications," in *Proceedings of the 2024 National Conference on Communications (NCC)*, (IEEE, 2024), 1–5.

3. D. K. Choudhary and R. K. Chaudhary, "A Compact via-Less Metamaterial Wideband Bandpass Filter Using Split Circular Rings and Rectangular Stub," *Progress in Electromagnetics Research Letters* 72 (2018): 99–106.

4. Z. Fu, X. Zou, Y. Liao, G. Lai, Y. Li, and K. L. Chung, "A Brief Review and Comparison between Transmitarray Antennas, Reflectarray Antennas and Reconfigurable Intelligent Surfaces," in *Proceedings of the 2022 IEEE Conference on Telecommunications, Optics and Computer Science (TOCS)*, (IEEE, 2022), 1192–1196.

5. J. Hu, S. Bandyopadhyay, Y.u-h. Liu, and L.i-y. Shao, "A Review on Metasurface: From Principle to Smart Metadevices," *Frontiers in Physics* 8 (2021): 586087.

6. H. Ojukwu, B. Seet, and S. U. Rehman, "Wideband and Load-Insensitive Metasurface Absorber for Radio Frequency Energy Harvesting," in *Proceedings of the 2022 IEEE 33rd Annual International Symposium on Personal, Indoor and Mobile Radio Communications (PIMRC)*, (IEEE, 2022), 963–967.

7. X. Song and W. Zhu, "Reconfigurable Metasurface for Dynamical Modulation of Reflection, Transmission, and Absorption," in *Proceedings of the 2021 IEEE International Symposium on Antennas and Propagation and USNC-URSI Radio Science Meeting (APS/URSI)*, (IEEE, 2021), 1221–1222.

8. S. Taravati, B. A. Khan, S. Gupta, K. Achouri, C. Caloz, "Nonreciprocal Nongyrotropic Magnetless Metasurface," *IEEE Transactions on Antennas and Propagation* 65, no. 7 (2017): 3589–3597.

9. W. Yang, J. Qin, J. Long, et al., "A Self-Biased Non-Reciprocal Magnetic Metasurface for Bidirectional Phase Modulation," *Nature Electronics* 6 (2023): 225–234.

10. F. Ahmed, T. Tamoor, T. Hassan, N. Shoaib, A. Alomainy, and Q. H. Abbasi "Design and Development of a Multi-Functional Bi-Anisotropic Metasurface With Ultra-Wide Out of Band Transmission." *Scientific Report* 11, no. 1 (2021): 24244.

11. K. Takahagi and A. Tennant, "Experimental Verification of Nonreciprocal Electromagnetic Metasurface in a Finite-size Array," *Electronics Letters* 60, no. 12 (2024): e13240.

12. K. Takahagi and A. Tennant, "Experimental Validation of Nonreciprocal Metasurface Using Simple Structure," *The Journal of Engineering* 10 (2024): e70011.

13. A. Parsa, T. Kodera, and C. Caloz, "Ferrite Based Non-Reciprocal Radome, Generalized Scattering Matrix Analysis and Experimental Demonstration," *IEEE Transactions on Antennas and Propagation* 59, no. 3 (2011): 810–817.

14. N. Marcuvitz, "Gratings and Arrays in Free Space," in *Waveguide Handbook* (New York: McGraw-Hill, 1951), 284–286.